ISSN 0742-0463, Journal of Volcanology and Seismology, 2026, Vol. 20, No. 2, pp. 190–203. © Pleiades Publishing, Ltd., 2026.

Formation Conditions and Geothermal Resources of the Paratunka Geothermal Fields

A. V. Kiryukhin[a, b, *], **N. B. Zhuravlev**[a], **S. V. Alekseenko**[c], **S. L. Elistratov**[b, c], **and D. N. Burnaykin**[d]

[a] *Institute of Volcanology and Seismology, Far East Branch, Russian Academy of Sciences, Petropavlovsk-Kamchatsky, 683023 Russia*

[b] *Vitus Bering Kamchatka State University, Petropavlovsk-Kamchatsky, 683023 Russia*

[c] *Institute of Thermophysics, Siberian Branch, Russian Academy of Sciences, Novosibirsk, 630090 Russia*

[d] *JSC Teplo Zemli, Termalny, Kamchatka krai, 684035 Russia*

**e-mail: AVKiryukhin2@mail.ru*

Received October 28, 2025; revised October 28, 2025; accepted December 26, 2025

Abstract—The Paratunka and Verkhny Paratunsky deposits (Kamchatka, Russia) are examples of worldwide widespread low-temperature nitrogen (LT N_2) geothermal systems. The Paratunka geothermal fields are located 15 km apart, composed of the Eocene–Quaternary volcanic rocks, and characterized by shallow permeable reservoirs with deep conductive roots inherited from extinct volcanoes with circulating SO_4–Na nitrogen thermal waters of 60–90°C. The Paratunka reservoir has a 60-year history of intense exploitation (150–250 kg/s), whereas the Verkhny Paratunsky reservoir is just being commissioned. A 3D numerical thermohydrodynamic model is developed for the Verkhny Paratunsky and Paratunka LT N_2 geothermal system (Kiryukhin et al., 2025), which suggests that the top of the pre-Cretaceous basement is permeable, whereas the roots of extinct volcanoes are the channels for thermal fluid upflows and thermal spring discharge. This numerical model also includes a water recharge area from adjacent highlands. The feasibility of exploiting a potential deep reservoir confined to the structural surface of the pre-Cretaceous basement top (an area of 270 km^2) for heat supply and using the binary technologies for electric power generation is confirmed. According to numerical modeling results, the possible initial power generation is estimated at 32.3 MWe.

Keywords: heat mining, geothermal field, thermohydrodynamic modeling, Paratunka, 3D, LT, N_2, EWASG, binary technology

DOI: 10.1134/S0742046326700041

INTRODUCTION AND TASK FORMULATION

Low-temperature nitrogen geothermal (LT N_2) fields, which are defined by a reservoir temperature up to 150°C at depths of up to 1 km (Rybach, 1981; Axelsson, 2000; Johannesson, 2016; Kiryukhin et al., 2025), are typically dominated by nitrogen in gas composition, which indicates meteoric water feeding and the absence of magmatic heat sources. These deposits showed potential for long-term (decades) commercial exploitation in Iceland, Hungary, China (Zippa, 2020; Li et al., 2023; Peng et al., 2023), Turkey, France, Germany (Schill and Genter, 2003; Genter et al., 2016), Russia and the former USSR (Barabanov and Disler, 1969; Manukhin and Vorozheikina, 1976; Shvatrsev et al., 2016; Kharitonova, 2020, 2024; Polyak et al., 2022; Lyamina, 2022), Mongolia (Sumaazhav, 2022), Italy (Gherardi et al., 2000; Pola et al., 2015; Torresan et al., 2020), Serbia (Marinković et al., 2023), Mexico (Peiffer et al., 2024) and other countries (Fig. 1). This experience allowed the suggestion on formation mechanisms of such reservoirs including water and heat recharge conditions in natural environments (Bodvarsson, 1983; Shvatrsev et al., 2016) and during the operation and the estimation of their permeability-capacity properties and the degree of resource renewability (Axelsson, 2000; Kiryukhin et al., 2017, 2025). Numerical modeling substantiated principal mechanism of heat and water recharge of the LT N_2 hydrothermal fields, which requires a natural centripetal geocirculation system with an area of hundreds of square kilometers and the presence of fluid-conducting structural surfaces at depths of 3 km (Kiryukhin et al., 2025). This paper refines the above model and shows practical applications for the Paratunka geothermal fields.

HYDROGEOLOGICAL STRATIFICATION AND PRODUCTIVITY OF THE PARATUNKA AND VERKHNY PARATUNSKY DEPOSITS

Based on results of exploration drilling at the Paratunka geothermal field mostly to a depth of 2.5 km, it

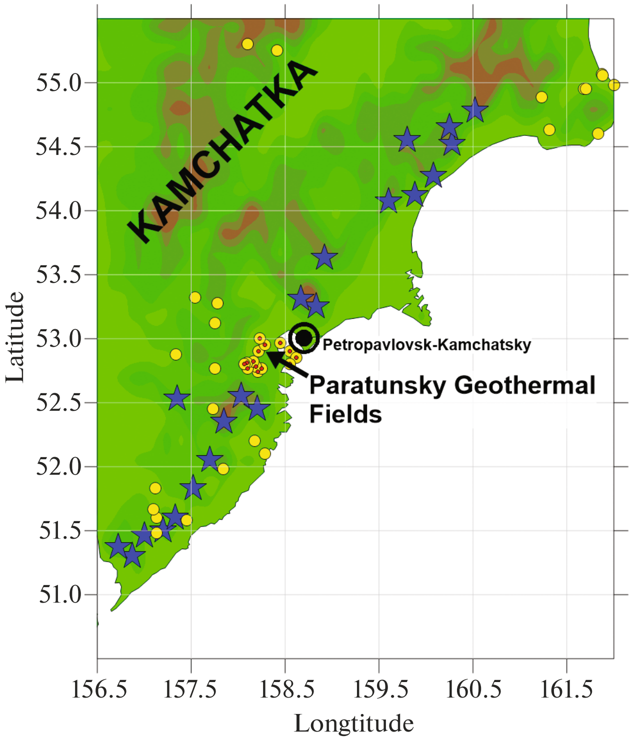

Fig. 1. Location of the Paratunka LT N_2 geothermal systems in Kamchatka. Yellow circles, discharges of the LT N_2 geothermal systems; inner red circle, the Paratunka system; blue stars, active volcanoes.

has the following hydrogeological stratification (Kiryukhin et al., 2017).

1. Alluvial sandy–gravel–pebble deposits with a strong flow of cold groundwater.

2. Lower Quaternary siltstone with interbeds of fine-grained sandstone 10–150 m thick (acting as a water- and heat-proof layer) at depths of 40–180 m.

3. Lower Quaternary conglomerate with interbeds of siltstone and tuffaceous sandstone forming the upper aquifer of thermal waters.

4. Tuff sandstone, tuff conglomerate, and tuff of the Alnei Group common only in the Northern area.

5. Tuffaceous–pyroclastic rocks of the Paratunka Formation characterized by the highest water content are the main thermal host rocks.

6. Intrusive rocks, which are slightly water-saturated excluding for certain tectonic zones.

Last four horizons are combined into a single confined thermal aquifer complex, hosted in fracture-vein and fracture-layer reservoir. The presence of a consistent relative caprock (the Lower Quaternary siltstone, sandstone, and clay) 10–100 m thick with a depth of the top at 40–80 m provides excess pressure of thermal water reservoir.

To analyze the relationship between the well productivity and depth, we used data from tops of productive zones penetrated during well drilling (confirmed by factual water inflows). A total of 398 productive zones with a total initial thermal fluid inflow of 1098 kg/s were identified at the field.

The correlations of the normalized flow rate for the wells of the Sredny, Lower, and Northern Sites of the Paratunsky geothermal field, respectively (the inflow from the interval to a given depth divided by a number of wells drilled to the indicated depth) show (Figs. 2a, 2b) no water inflows (groundwater (1) and upper aquifer (2)) in the upper part of the section at a depth from 0 to 100–150 m, an increase thermal water inflow to 3–4 kg/s (the upper conglomerate aquifer of thermal waters (3)) to a depth to 250–300 m and to 17.3–25.5 kg/s (0.014–0.021 kg/s/m, the tuffaceous complexes of thermal waters of the Alney Formation and Paratunka Formation (4–5)) deeper to 1200–1350 m, and a decrease to 4–3 kg/s (0.004–0.003 kg/s/m) at a depth of up to 2400–2500 m (complexes of thermal waters of the basement and intrusive rocks (6)).

A similar geological section was identified on the basis of exploration drilling at the Verkhny Paratunsky deposit to a depth of 1.5 km, therefore, it has a similar hydrogeological stratification.

1. Alluvial sandy and gravel–pebble deposits include cold groundwater.

2–3. Relative aquiclude (to a depth of the water inflow zone with a flow rate at the wellhead exceeding 1 kg/s) is 36–822 m (wells GK-19 and GK-37) mostly of 200–600 m.

4–5. Rocks of the Alney Formation (N al): mafic and intermediate lava and tuff, tuffaceous claystone, siltstone, sandstone, and conglomerate; Berezovskaya Formation (N_1 br): mostly mafic and intermediate lava and tuff, rhyolite, ignimbrite, as well as tuffaceous siltstone, claystone, sandstone, and conglomerate; Vilyuchinsk Formation (P_1–N_1 vl): tuffaceous claystone, siltstone, sandstone, conglomerate, tuffite, tuff, andesitic and basaltic lava. The thickness of some lithological varieties ranges from a few tens to hundreds of meters.

6. Intrusive rocks include diorite, quartz diorite, and granodiorite. The depth of the intrusive from the surface varies from 53 (well GK-25) to 1400 (well 86) m.

The last three horizons form a productive geothermal reservoir.

The correlation of the normalized flow rate (the inflow from an interval to a given depth divided by a number of wells drilled to the indicated depth) at the Verkhny Paratunsky field is shown in Fig. 2c. The normalized well flow rate is 9 kg/s (0.015 kg/s/m) in the upper part of the section from –500 m to 100 m, 15 kg/s (0.041 kg/s/m) in a depth from –870 to –500 m, and 3.4 kg/s (0.006 kg/s/m) from –1400 to –870 m. This indicates significant horizontal productivity of horizons 4–6, especially, in the middle part (the interval from –870 to –500 m).

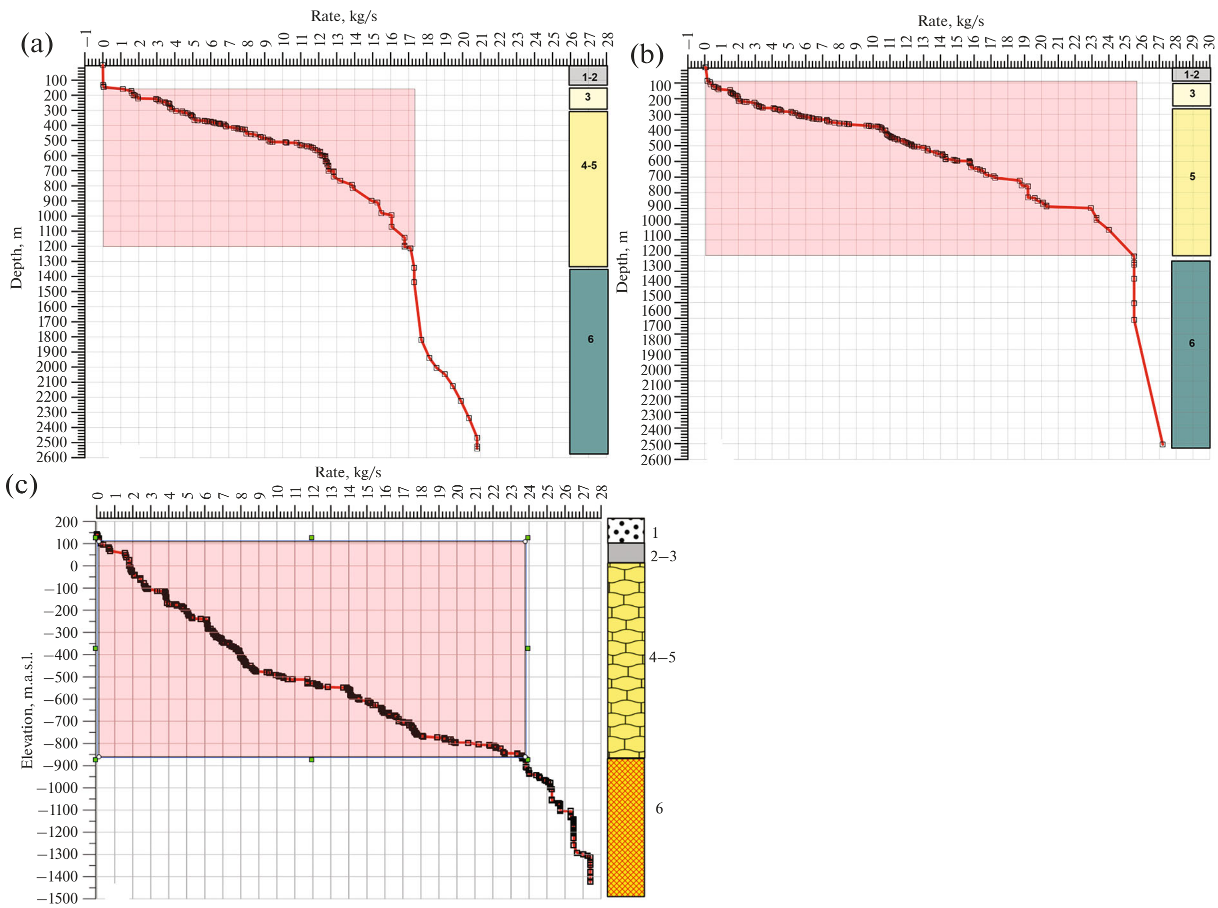

Fig. 2. Correlation between normalized geothermal well flow rate and the depth for the Sredny Site (a) and the Lower and Northern Sites (b) of the Paratunsky geothermal field (Kiryukhin et al., 2017) and the Verkhne-Patayunsky geothermal field (Kiryukhin et al., 2025) (c). 1, Alluvial deposits; 2, Lower Quaternary siltstone with fine-grained sandstone interbeds (the upper caprock); 3, Lower Quaternary conglomerate; 4, tuffaceous sandstone, tuffaceous conglomerate; 5, tuffaceous-pyroclastic rocks of the Alney, Paratunka, Berezovskaya, and Vilyuchinsk formations; 6, intrusive rocks. Red rectangles show the most productive intervals.

3D DISTRIBUTION OF TEMPERATURE AND PRODUCTIVITY

The initial 3D temperature distribution of the Verkhny Paratunsky and Paratunka geothermal fields was calculated from well bottom temperature registered during drilling after a long recovery period. The initial data included 117 wells and 517 data points (2016 well catalogs of the JSC Teplo Zemli). The Green module from the LIDA-3 data approximation library (Kiryukhin, 1993) was used for the 3D spline approximation of initial temperature data. The calculations were performed with an acceptable standard deviation of the spline from a factual temperature of 1°C. A 44 × 60 × 10 grid of points was defined for the calculations of temperature distribution on a 3D area of 22 km × 30 × 2.5 km.

The temperature distribution (at the –750 m level) within the Verkhny Paratunsky and Paratunka geothermal fields is shown in Fig. 3.

The temperature anomaly of the Verkhne-Paratunsky field outlines two productive reservoirs: a large of 9 km × 4 km in size (eastern Site, NW strike) and a small of 1.5 km × 1.5 km in size (western Site, Karymshinsky) and coincides with geoisotherm of 60°C. The temperature anomalies at the Paratunka deposit outline the following productive reservoirs along the geotherm of 70°C: SR (6 km × 1 km, nearly longitudinal), NP + N (7 km × 1.5 km, nearly longitudinal), and M (1 km × 1 km).

Note that tectonic maps, which are used on geological maps, show faults, some of which are inactive and impermeable, i.e., capable of transporting thermal waters. Therefore, it is important to collect information on the distribution of productive plane-oriented faults/planes within the Paratunka and Verkhny Paratunsky geothermal fields based on factual thermal water inflow data, which were measured during the drilling of exploration and exploitation wells.

The analysis is based on the penetration of productive zones during well drilling confirmed by factual

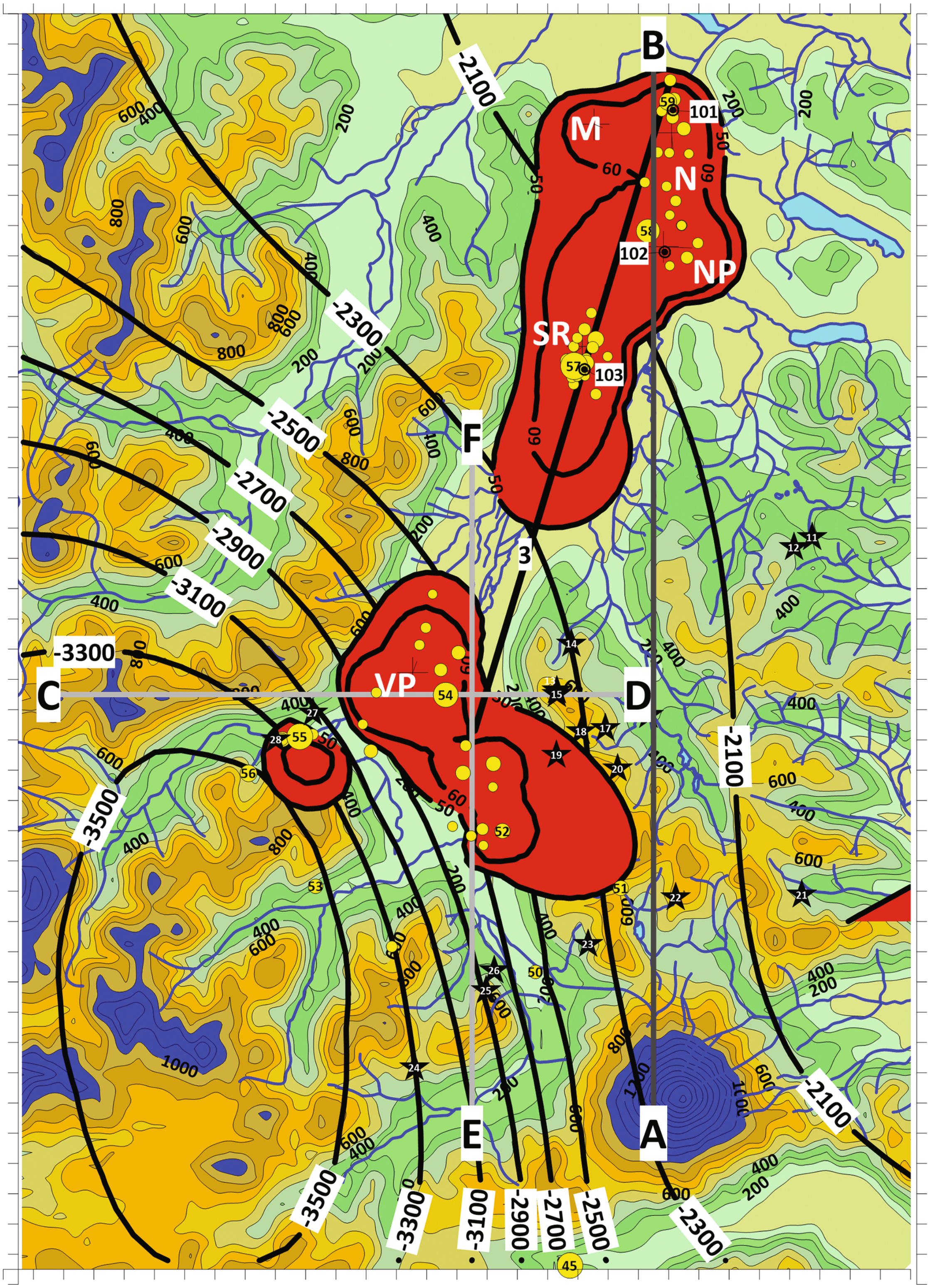

Fig. 3. Water recharge conditions of the Paratunka (SR, NP, N, M) and Verkhny Paratunsky geothermal fields. Blue areas, the water recharge areas above 1000 m abs. (represent extinct volcanic structures with high vertical permeability); red areas, the productive reservoirs contoured by 50 and 60°C isotherms at the level of –750 m; yellow circles, thermal (hot) springs; their sizes are proportional to the temperature and are numbered according to (Kiryukhin et al., 2010); yellow circles, the productive wells with an initial flow rate of >5 kg/s; their sizes are proportional to the flow rates; black stars with numbers inside, the monogenic Pleistocene–Holocene cinder cones (Bergal-Kuvikas et al., 2022); black isolines, the surface of the pre-Cretaceous basement top, black line with number "3" is a trace of production fault at –750 m abs (Kiryukhin et al., 2025). The map shows the AB, CD, and EF cross-section lines (see below) and position of three deep (2.5 km) wells (101, 102, and 103). Axes are marked at 1 km.

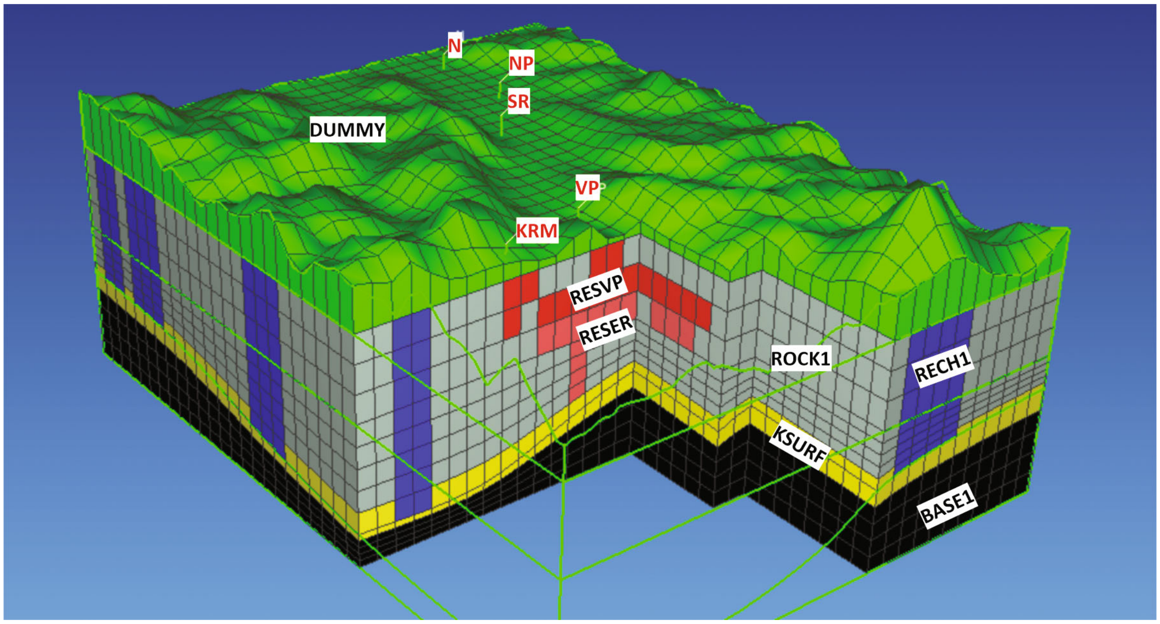

Fig. 4. 3D model zoning (black text) and hot spring discharges (red text). The material properties are given in (Kiryukhin et al., 2025).

water inflow data. A modified Frac-Digger2 algorithm for the plane-oriented clusters (Kiryukhin and Kiryukhin, 2017) was used to identify the clusters of productive zones that form 2D planes interpreted as productive faults or horizons.

In particular, the calculations in scenario ## 2 (Kiryukhin et al., 2025) considered the deep-well fluid inflow zones with high inflow rates (individual flow rates of >5.0 kg/s) and assumed the presence of long productive faults. This scenario used 108 water inflow zones including 62 and 46 zones, which are exposed in the Paratunka and Verkhny Paratunsky fields with a total deep-well fluid inflow of 676.4 and 471.2 kg/s, respectively. The selection criteria included δR = 30 km and δZ = 100 m (the deviation from the calculated plane).

As a result, the following thermal conductive structures are identified: 1) two almost horizontal production planes at depths of –601 m and –386 m and 2) a productive fault (a dip angle of 68° in a SEE direction), which likely connects the Verkhny Paratunsky and Paratunka productive reservoirs. The trace of the productive fault (a dip angle of 68°, a dip azimuth of 107°, and production of 66 kg/s) at the depth of –750 m is shown as ##3 in Fig. 3.

FULL-SCALE 3D THERMOHYDRODYNAMIC MODEL OF THE VERKHNY PARATUNSKY AND PARATUNKA HYDROTHERMAL SYSTEMS AND ITS APPLICATIONS

Brief Model Description

The assembly of the 3D thermohydrodynamic (TH) model of the Paratunka hydrothermal systems is described in details in (Kiryukhin et al., 2025); below, we briefly provide its main characteristics (Fig. 4).

The model of the formation of the Paratunka and Verkhny Paratunsky LT N_2 hydrothermal systems suggests deep descending flows (to 3–4 km) of meteoric waters in the water recharge areas (Vilyuchinsky volcano and surrounding high-mountain structures (Kiryukhin et al., 2017, Fig. 12B)), their further transit and simultaneous heating to 100–110°C due to the heat exchange with host rocks, and the formation of an ascending thermal water flow feeding the productive geothermal reservoir. It is suggested that the upper part of the pre-Cretaceous basement is a permeable contact surface (Fig. 3) favorable for the regional lateral fluid flows, whereas magmatic roots of extinct volcanic structures (Vilyuchinsky volcano, Sopka Goryachaya volcano, and a volcano in the SR site) work as highly permeable channels for the vertical fluid transport.

The model geometry includes the area of the Paratunka River valley and adjacent volcanic highlands (Fig. 3) with an area of 29.0 × 38.0 km, which in cross-section covers a vertical range from –4000 m to the topographic surface. Thus, the model covers all significant thermal manifestations (VP, KRM, SR, NP, and N hot springs) and water supply areas (Vilyuchinsky volcano and highlands above 1000 m abs.).

Using the TOUGH2 with the EWASG fluid state module describes the thermal waters as a three-component (water, NaCl, and N_2) single-phase fluid. The modeling used a four-layer (14 sublayers) rectangular regular 3D computational grid measuring 29 × 38 × 14 with a horizontal base element size of 1000 × 1000 m.

Layer 1 (upper layer) is given in a range of heights from 0 m to the topographic surface. Layer 2 includes three sublayers 500 m thick each ranging from −1500 m to 0 m. Layer 3 includes five sublayers ranging from the upper part of the pre-Cretaceous basement (Fig. 3) to −1500 m. Layer 4 includes five sublayers ranging from −4000 m to the upper part of the pre-Cretaceous basement. Thus, the total number of the model elements was 15428.

The model zoning (Fig. 4) includes the following domains: ROCK1 is the host rocks consisting of low-permeable Tertiary volcanic and sedimentary rocks; RECH1 is a domain beneath the water supply area of the Vilyuchinsky volcano and uplands above 1000 m with the given boundary conditions of infiltration; BASE1 is the deep low-permeable pre-Cretaceous basement; DUMMY is an area of the upper layer 1 necessary for reproducing the conductive heat losses and low permeability is assigned to prevent the occurrence of mass flows; KSURF is a possibly permeable domain 500 m thick representing the contact zone of the pre-Cretaceous basement, which includes the upper sublayer of layer 4 and the lower sublayer of layer 3; RESER is a domain representing the volume of active circulation without specific productive reservoirs; and RESVP, RESSR, RESNP, RESNN, and RESYZ are the exploitation reservoirs: Verkhny Paratunsky, SR area, NP area, Paratunka area N, and South Berezhny area, respectively.

Inversion modeling based on initial temperature and pressure distribution data and exploitation history from 1964 to 2014 was used to assess the reservoir properties of the productive geothermal reservoir. According to the results of the iTOUGH2 inversion modeling, the values of horizontal permeability of up to 1.41 D, vertical permeability of 168 mD, and compressibility of up to 4.08×10^{-8} Pa^{-1} are most reasonable. The total natural deep ascending flow is estimated at 190 kg/s at a temperature of 80–111°C (Kiryukhin et al., 2017). The permeability of the productive reservoirs decreases exponentially as the temperature drops below 70°C. This was taken into account in the detailed zoning of the model: the permeability decreases by a factor of 10 in a temperature range of 65–70°C and by an additional order of magnitude in a range from 60 to 65°C.

Single-phase initial conditions corresponding to buried seawater (salinity of 10 g/L) at the hydrostatic pressure distribution and the temperature gradient of 25°C/km were given in the model (Kiryukhin et al., 2025). In this study, the initial geothermal gradient increased to 30°C in the model taking into account geothermometer data (SiO_2, Na–K, and Na–K–Ca; Kiryukhin et al., 2017) indicating a basic temperature of 105–115°C, as well as geological indicators of recent magmatic activity (Bergal-Kuvikas et al., 2022).

The conditions of the meteoric water influx were given in the RECH1 domain (Fig. 4) as the boundary condition with a constant pressure and the hot spring discharges were defined as "well on deliverability wells" in the five model elements corresponding to the most significant thermal discharges (VP, KRM, SR, NP, and NN) (Fig. 4). Discharge to the Avacha Bay was given using the fixed-state boundary condition at the eastern boundary of the model.

Natural State Modeling

Natural state modeling was conducted for a circulation period of up to 50000 years and showed the possible long-term circulation with a total discharge of ~245 kg/s, a temperature of up to 80°C, and a salinity of 0.55 g/L. This corresponds to expected parameters of the Paratunka hydrothermal systems. Figures 5 and 6 show spatial distribution of temperature and NaCl concentration throughout the hydrothermal system at the moment of 5000 years from the circulation onset: the productive reservoirs and their roots warmed to 60°C and more, whereas the intermediate saline areas were diluted.

The spatial temperature distribution (Fig. 5) clearly explains the circulation structure and the gradual heat mining mechanism in the LT N_2 geothermal systems: 1) the descending flow of cold meteoric waters from the elevated recharge areas to the surface of the pre-Cretaceous basement top; 2) the transition to horizontal/subhorizontal flows along the structural surface (500 m thick) at a depth from −3.5 km to −2 km over an area of 1100 km^2; 3) the formation of ascending heated water flows along the roots of extinct subvolcanic structures; and 4) the formation in shallow reservoirs with a temperature of 60°C and discharge in productive areas (N, NP, SR, VP, KR, an d KRM) within the Paratunka River valley. Thus, the heat supply is provided by two heat mining mechanisms: due to the heat capacity of permeable reservoirs with circulation and due to heat removal from the host rocks, which is caused by regional component of the conductive heat flow (estimated at ~60 MW/m^2) and heat capacity of the host rock itself.

The 3D distribution of the NaCl concentration in Figure 6 indicates a reason of generally low salinity of the LT N_2 geothermal systems. This is due to dilution of initially burried sea waters (10 g/kg) by infiltrated meteoric waters and their transformation to low-saline water (<1 g/kg).

MODELING APPLICATION FOR THE ESTIMATION OF ELECTROGENERATION FROM THE DEEP RESERVOIR (TOP OF THE PRE-CRETACEOUS BASEMENT)

3D modeling can practically be valuable for the development of exploration well drilling strategies and sustainable increase in their production. Most wells at

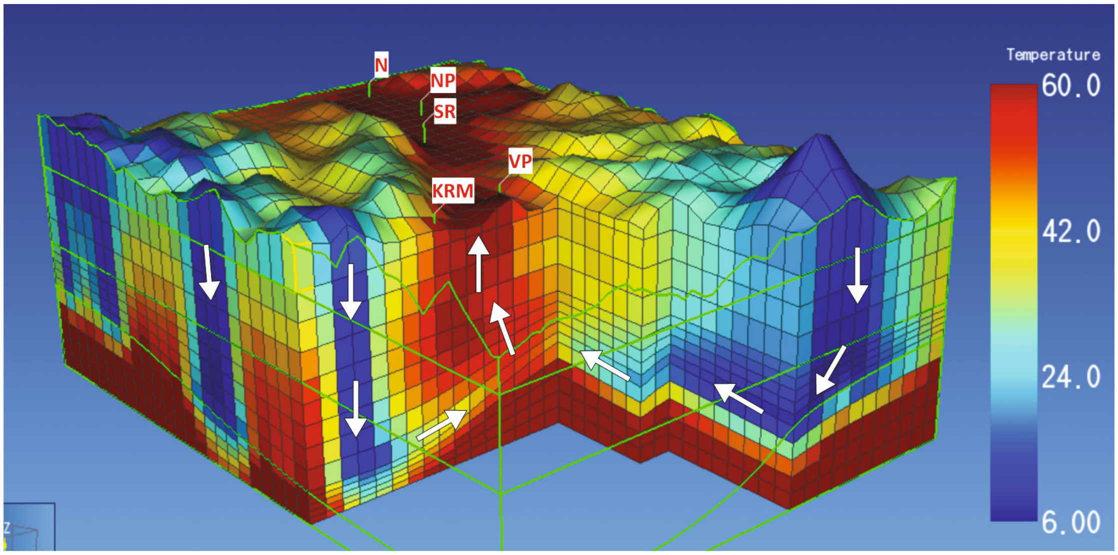

Fig. 5. Natural state run (scenario ##5). 3D temperature distribution at the moment of 50 000 years. Here and in Fig. 6, red text, the location of hot springs; white arrows, the main fluid flows.

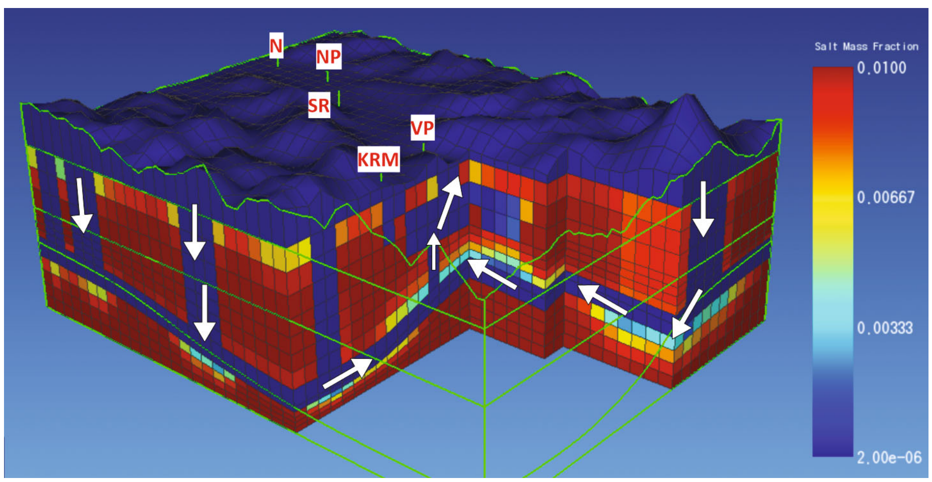

Fig. 6. Natural state run (scenario ##5). 3D NaCl distribution (in mass fractions) at the moment of 50 000 years.

the Paratunka and Verkhny Paratunsky geothermal fields are between 100 and 1500 ms deep and three wells at the Paratunka field are 2.5 km deep (Fig. 3). Two of these wells are shown in Fig. 7a with Paratunka and Verkhny Paratunsky fields in the nearly-longitudinal cross-section. The dilution zone of the initial mineralized waters with the NaCl concentration of 400 ppm at a depth of ~2.3 km was formed by the meteoric water influx along the top of the pre-Cretaceous basement, which is identified in the model as a structural surface with relatively high permeability.

Figure 7a shows that both deep wells exposed a permeable structural zone at a depth of –2.5 to –2.0 km and provided an average flow rate increase of 3.5 kg/s from this interval (Fig. 2b). The bottomhole temperature of these wells (83 to 96°C) corresponds to modeling results (Fig. 7). The latter may indicate the presence of residual heat from extinct magmatic activity (roots of the extinct volcanoes and magmatic systems of the monogenic cinder cones (Bergal-Kuvikas et al., 2022)).

Thus, the pre-Cretaceous structural surface with a potentially exploited geothermal reservoir of an area of 270 km^2 (Figs. 7, 8) can be drilled with possible additional heat extraction using innovative heat exchanger systems (Zayed et al., 2023; Rajeh et al., 2024; Al-Kbodi et al., 2023), in particular, coaxial geothermal systems with packers (Yin et al., 2024) or others.

Let us consider at first approximation the possible electric power generation from the deep target reservoir of the Paratunka hydrothermal systems (Fig. 8) using isobutane-based binary technologies (Fig. 9).

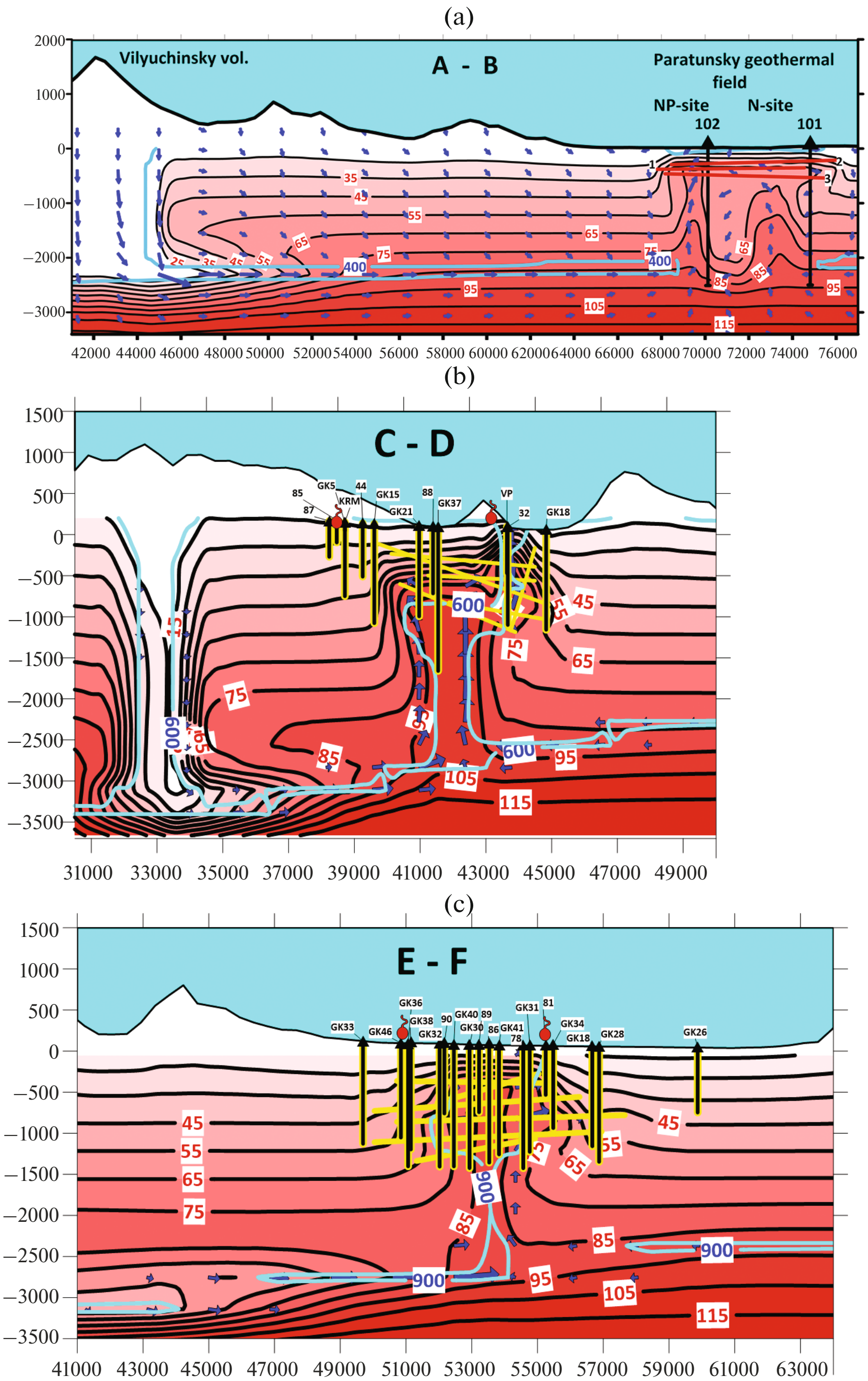

Fig. 7. A–B (a), C–D (b), and E-F (c) cross-sections of the 3D TH model (scenario ##5). All figures: red marks, temperature, °C; blue marks, NaCl distribution, ppm. (a) 1, 2, 3, the productive shallow reservoirs; blue arrows, vectors proportional to the thermal fluid flow rates at the moment of 5000 years (natural state run, scenario ##5); deep wells 101 and 102 are also shown; the position of A–B cross-section is shown in Fig. 3; (b) blue arrows, vectors proportional to the thermal fluid flow rates at the moment of 5000 years (natural state run, scenario ##5); the position of C–D cross-section is shown in Fig. 3; (c) blue arrows, vectors proportional to the thermal fluid flow rates at the moment of 5000 years (natural state run, scenario ##5); the position of E–F cross-section is shown in Fig. 3.

The potential energy production from the target reservoir of the top of the pre-Cretaceous basement is estimated with multivariate TOUGH2 numerical modeling using the five-point exploitation scheme, which is distributed across each element of the target reservoir model (KSURF) shown in Fig. 8 taking into account the available for drilling geothermal resource at up to 400 m abs. The material properties of the cal-

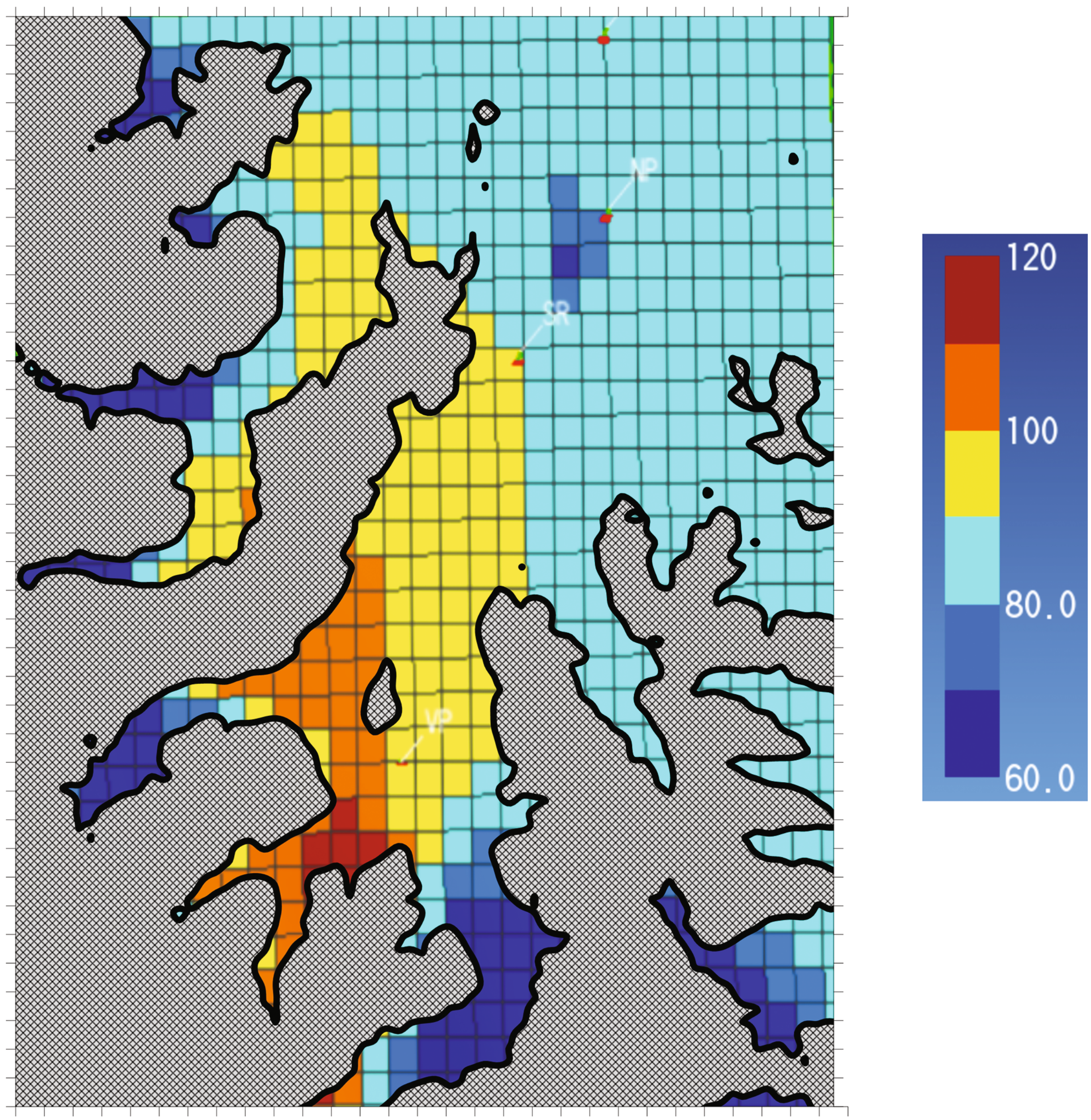

Fig. 8. Temperature distribution in the deep target reservoir suggested on the top of the pre-Cretaceous basement structural surface according to the 3D TH modeling results (scenario ##5). The accessible area of the target reservoir with temperatures of >100°C is 25 km^2 (25 model elements), whereas the area with temperatures of >110°C is 4 km^2 (four model elements). The area with topo elevations above 400 m abs. is shaded.

culation blocks were given as in the KSURF domain (Kiryukhin et al., 2025, Table 4). Each model element was divided into four identical calculation blocks with a conductive heat flux of 60 mW/m^2 at each base and the initial temperatures were given according to Fig. 8. The center of each calculation block contained an injection well with a flow rate of Q and an enthalpy of 159 kJ/kg (38°C correspond to the condensation temperature of the coolant under climate conditions of an uninterruptible summer air condenser) and water withdrawal with a flow rate of Q/4 was given at four apices of the circulation system square (Fig. 10).

Modeling was conducted for a period of 30 years from the start of the circulation system operation at the flow rates of 30–60 kg/s with an increment of 10 kg/s and initial temperatures of 100 and 110°C.

The electric power generation capacity from one calculation block of the target reservoir was calculated from the circulation flow rate Q and the temperature

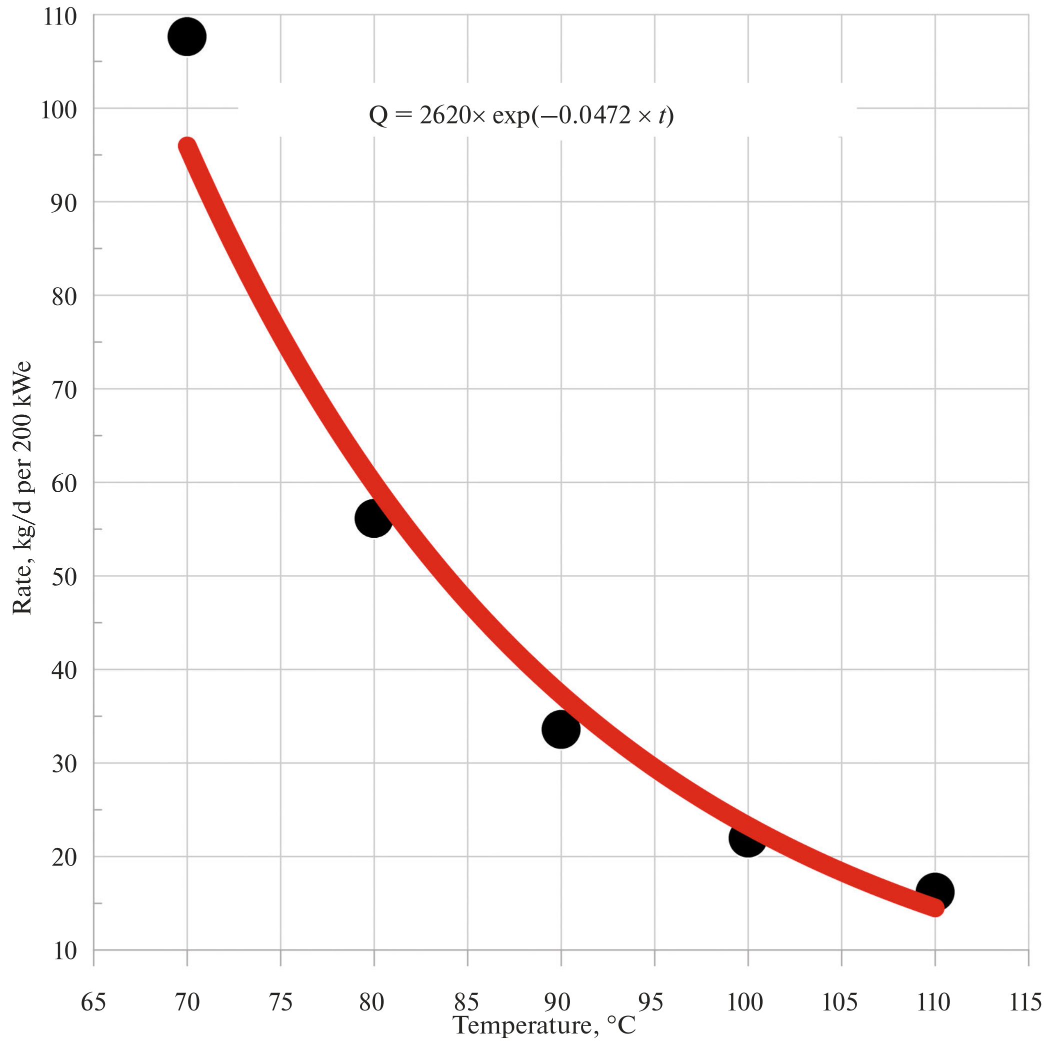

Fig. 9. Hot water demand (kg/s) for generating the 200 kW electrical energy as a function of initial water temperature *t* for the Rankine cycle on isobutane R600a.

correlation of hot water demand for electric power generation (Fig. 9):

$$We = 0.0763Q\exp(0.0472t), \quad (1)$$

where *We* is the estimated electric power, kW; 0.0763 is the coefficient, kW/kg/s; *Q* is the circulation system flow rate, kg/s; *t* is the well outlet temperature, °C.

Modeling showed that the increase in the flow rate of the five-point circulation system leads to enhancing temperature decrease in the production circuit and, as a result, a decrease in electricity generation (*We*). At the circulation system flow rate of 30 kg/s, the rate of temperature decrease in the production circuit is minimal (2.1 and 2.4°C) at the initial block temperatures of 100 and 110°C, respectively, over 30 years of operation (Fig. 11). At the initial electric power generation of 0.41 MW e (110°C) and 0.26 MW e (100°C), its decreases to 0.37 MW e and 0.23 MW e, respectively.

The calculation of the total electric power generation from the target reservoir (Fig. 8) at a flow circulation rate of 30 kg/s and taking into account the available geothermal resource at the topographic heights of up to 400 m abs. is shown in Table 1. Thus, the deep productive reservoir (the top of the pre-Cretaceous basement) can provide the initial production of 32.3 MW e with a decrease in its total generation to 29.1 MW e over the next 30 years.

CONCLUSION

The Paratunka and Verkhny Paratunsky geothermal fields (Kamchatka, Russia) are examples of worldwide widespread low-temperature nitrogen (LT N_2) geothermal systems, which formed as a result of meteoric water infiltration to deep 3D structures and heat mining from host rocks at the background heat flow and temperature gradients.

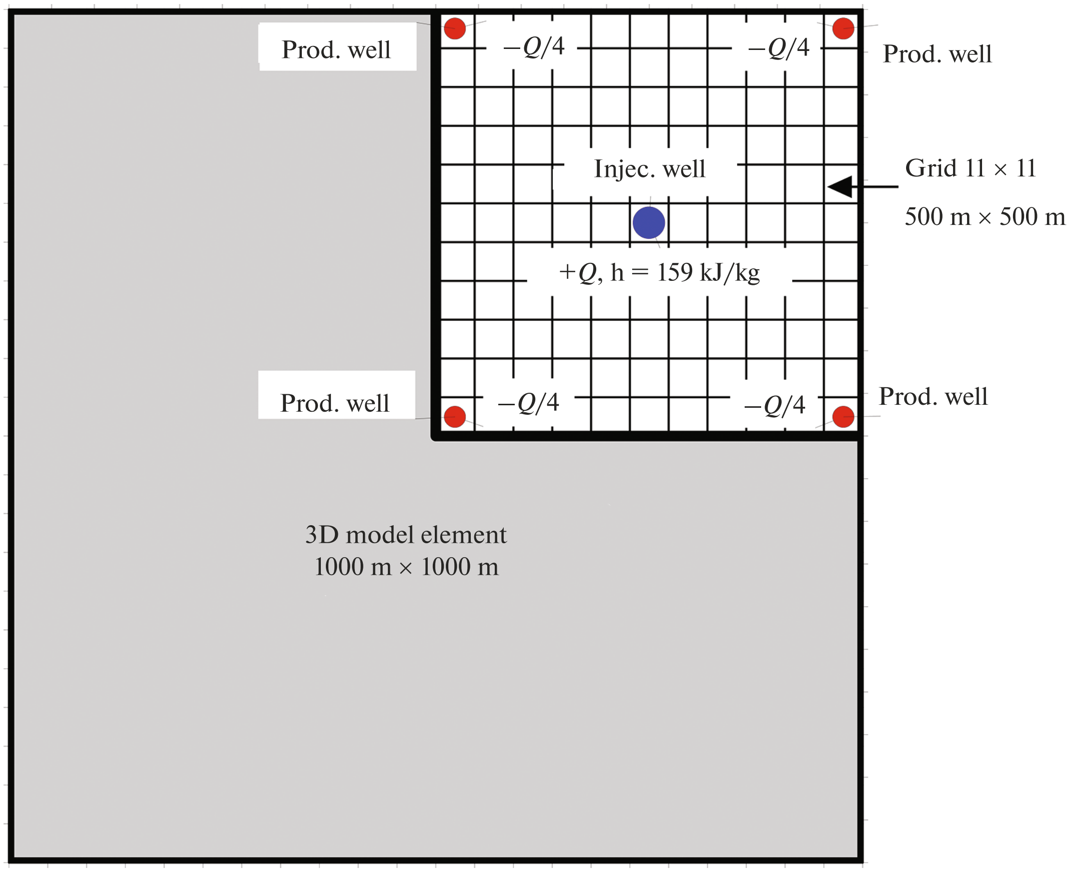

Fig. 10. Calculation scheme of the local five-point circulation system for heat extraction for a single element of the target reservoir 3D model (Fig. 8).

The Paratunka geothermal fields are located 15 km apart, composed of the Eocene–Quaternary volcanogenic-sedimentary rocks, and characterized by shallow permeable reservoirs with deep conductive roots from extinct volcanoes and circulation of nitrogen SO_4–Na thermal waters at temperatures of 60–90°C. The Paratunka reservoir has a 60-year history of intense production (150–250 kg/s), whereas the Verkhny Paratunsky reservoir is just about the exploitation.

This study uses a 3D numerical thermohydrodynamic model of the Verkhny Paratunsky and Paratunka LT N_2 geothermal systems, which suggests that the top of the pre-Cretaceous basement is permeable and the roots of extinct volcanoes provide channels for deep heat exchange and discharge of thermal springs. This numerical model also includes a water recharge areas from the adjacent highlands. Modeling confirms possible long-term hydrothermal circulation at a temperature of ~80°C and a thermal fluid flow rate of 245 kg/s and dilution of primary seawater from 10 to 0.5 g/L (NaCl).

The structural surface of the top of the pre-Cretaceous basement is considered a target productive geothermal reservoir (an area of 270 km^2 and a thickness of 500 m according to modeling results) potentially

Table 1. Calculation of total electric power generation from the target reservoir with a temperature of >100°C on the top of the structural surface of a pre-Cretaceous basement (Fig. 8) using five-point (Fig. 10) circulation system for thermal fluid extraction with a flow rate of 30 kg/s over a 30-year period of operation

			Total
Temperature of calculation block, °C	100	110	
Number of blocks of five-point circulation system	100 = 25 × 4	16 = 4 × 4	
Total initial electric generation, MW e	25.7 = 100 × 0.257	6.6 = 16 × 0.41	32.3
Total final electric generation, MW e	23.2 = 100 × 0.232	5.9 = 16 × 0.37	29.1

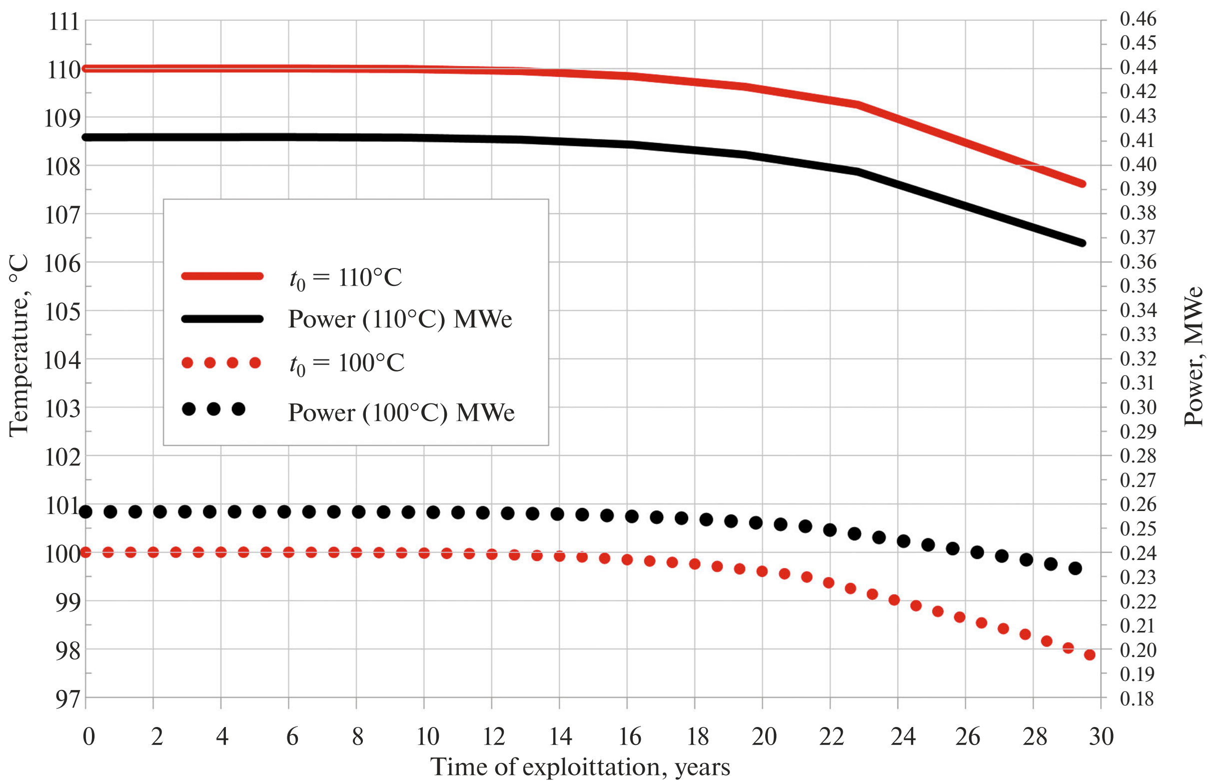

Fig. 11. Forecasted temperature and power generation changes at the outlet of production wells in the five-point circulation system over 30 years for two modeling options (with initial temperatures t_0 = 110°C and t_0 = 100°C) at the circulation rate of Q = 30 kg/s.

suitable for exploitation. Its use is possible by means of intensificated technology, coaxial geothermal systems or other new heat exchanger systems. Electric power generation is also possible using binary technologies.

The multivariate numerical TOUGH2 modeling estimated the electric power generation potential from the target reservoir on the top of the pre-Cretaceous basement (29 km^2) at a temperature of >100°C. Using the five-point circulation system for the fluid extraction with the flow rate of 30 kg/s and the Rankine cycle using R600a isobutane, it is possible to achieve the initial electric power generation of 32.3 MW e decreasing to 29.1 MW e over 30 years of operation.

ACKNOWLEDGMENTS

We are grateful to L.E. Pavlova, A.V. Sergeeva, O.V. Bergal-Kuvikas, N.P. Asaulova, and N.V. Obora for data preparation, discussion, and interpretation of results, P.O. Voronin for supporting the field works, and P.A. Kiryukhin for technical support with Frac-Digger2. We also thank the anonymous reviewers for valuable comments, which helped us to improve the manuscript.

FUNDING

This work was supported by the Interdepartmental Program for Integrated Scientific Studies of the Kamchatka Peninsula and Adjacent Waters, which is implemented by the Vitus Bering Kamchatka State University under the project "Research and Modeling of the Life Cycle of Renewable Energy Facilities in Kamchatka Krai" (FZSS-2025-0008).

CONFLICT OF INTEREST

The authors of this work declare that they have no conflicts of interest

REFERENCES

Al-Kbodi, B.H., Rajeh, T., Li, Y., Zhao, J., Zhao, T., and Zayed, M.E., Heat extraction analyses and energy consumption characteristics of novel designs of geothermal borehole heat exchangers with elliptic and oval double U-tube structures, *Applied Thermal Engineering,* 2023, vol. 235, 121 418

Arnason, B., Hydrothermal systems in Iceland traced by deuterium, *Geothermics*, 1976, vol. 5, nos. 1/4, pp. 71–81.
https://doi.org/10.1016/0375-6505(77)90015-3

Axelsson, G., Gunnlaugsson, E., Jonasson, Th., and Olafsson, M., Low temperature geothermal utilization in Iceland—Decades of experience, *Geothermics,* 2010,

vol. 39, pp. 329–338.
https://doi.org/10.1016/j.geothermics.2010.09.002

Barabanov, L.N. and Disler, V.N., *Nitrogen Therms of the USSR,* Ministry of Health of the USSR, Central Institute of Balneology and Therapy, Moscow, 1968.

Bergal-Kuvikas, O., Bindeman, I., Chugaev, A., et al., Pleistocene-Holocene monogenetic volcanism at the Malko-Petropavlovsk zone of transverse dislocations on Kamchatka: Geochemical features and genesis, *Pure and Applied Geophysics,* 2022, vol. 179, pp. 3989–4011.
https://doi.org/10.1007/s00024-022-02956-7

Bodvarsson, G., Temperature/flow statistics and thermodynamics of low temperature geothermal systems in Iceland, *Journal of Volcanology and Geothermal Research,* 1983, vol. 19, pp. 255–280.
https://doi.org/10.1016/0377-0273(83)90114-2

Finsterle, S., *iTOUGH2 V7.0 Command Reference*, Rep. LBNL-40041 rev., Lawrence Berkeley Natl. Lab., Berkeley, California, 2014.

Fournier, R.O., Application of water chemistry to geothermal exploration and reservoir engineering, in *Geothermal Systems. Principle and Case Histories,* Rybach, L. and Muffler, L.J.P., Eds., J. Wiley and Sons, 1981, pp. 109–143.

Genter, A., Baujard, C., Cuenot, N., et al., Geology, geophysics and geochemistry in the Upper Rhine Graben: The frame for geothermal energy use, in *European Geothermal Congress 2016* Strasbourg, France, 19–24 September 2016, 2016.

Gherardi, F., Panichi, C., Caliro, S., Magro, G., and Pennisi, M., Water and gas geochemistry of the Euganean and Berician thermal district (Italy), *Applied Geochemistry,* 2000, vol. 15, pp. 455–474.
https://doi.org/10.1016/S0883-2927(99)00056-6

Kharitonova, N.A., Baranovskaya, E.I., Chelnokov, G.A., Bragin, I.V., Aseeva, A.V., and Karabtsov, A.A., Geochemistry and genesis of thermal waters of Northwestern Central Asia, in *Proceedings on the XXIV All-Russia Conference on Groundwater of the East of Russia*, Yekaterinburg, 2024, pp. 64–68. igduran.ru/files/eshop/elibrary/2024_podzemnaya_gidrosfera.pdf.

Kiryukhin, V.A., *Regional Hydrogeology*, St. Petersburg: Publishing House of the Mining Institute, 2005.

Kiryukhin, A.V., *Geothermofluidomechanics of Hydrothermal, Volcanic and Hydrocarbon Systems*, St. Petersburg: Eko-Vector I-P, 2020. elibrary.ru/item.asp?id=45739830.

Kiryukhin, A.V., High temperature fluid flows in the Mutnovsky hydrothermal system, Kamchatka, Geothermics, 1993, vol. 23, no. 1, p. 49–64.

Kiryukhin, P.A. and Kiryukhin, A.V., *Frac-Digger2.* Certificate of state registration of computer programs # 2017618050 as of September 21, 2017.

Kiryukhin, A.V. and Zhuravlev, N.B., Modeling of the formation conditions of nitrogen hydrothermal systems, in *Proceedings of the XXIV All-Russia Conference on Groundwater of the East of Russia*, Yekaterinburg, pp. 274—279. igduran.ru/files/eshop/elibrary/2024_podzemnaya_gidrosfera.pdf.

Kiryukhin, A.V., Yampolsky, V.A., Modeling Study of the Pauzhetsky Geothermal Field, Kamchatka, Russia, *Geothermics*, 2004, vol. 33, no. 4, pp. 421–441.

Kiryukhin, A., Lavrushin, V., Kiryukhin, P., Voronin, P., "Geofluid Systems of Koryaksky-Avachinsky Volcanoes (Kamchatka, Russia)," *Geofluids*, 2017, vol. 2017, Article ID 4279652.

Kiryukhin, A.V., Vorozheikina, L.A., Voronin, P.O., and Kiryukhin, P.A., Thermal-Permeability structure and recharge conditions of the low temperature Paratunsky geothermal reservoirs, Kamchatka, Russia, *Geothermics*, 2017, vol. 70, pp. 47–61.

Kiryukhin, A.V., Zhuravlev, N.B., Burnaikin, D.N., and Tokarev, I.V., Conceptual numerical modeling of low-temperature nitrogen geothermal systems on the Verkhne-Paratunsky and Paratunsky fields, *Geothermics,* 2025, vol. 131, 103 341.

Kononov, V.I., *Geochemistry of Thermal Waters in Modern Volcanic Areas,* Moscow: Nauka, 1983.

Kuzmina, E.A., *Relationship between Nitrogenous Thermal Waters and Fault Tectonics of the Barguzin-Bauntov Branch of the Baikal Rift System Basins, Cand. Sci. (Geol.-Mineral.) Dissertation,* Irkutsk, 2023, 230 p. crust.irk.ru/images/upload/newsfull229/3851.pdf.

Li, Y.M., Formation of the hydrothermal system from granite reservoir for power generation in igneous rock areas of South China, *Geothermics,* 2023, vol. 110, 102 673.
https://doi.org/10.1016/j.geothermics.2023.102673

Lyamina, L.A., *Hydrogeological conditions of formation of low-enthalpy mineral waters in crystalline rock massifs (on the example of Kuldur field, Jewish Autonomous Region), Cand. Sci. (Geol.-Mineral.) Dissertation,* Moscow, 2022, 162 p. dissovet.msu.ru/download/1c0ad192-70bb-11ed-81d7-005056b93961.

Maltseva, K.I., Nazhalova, I.N., and Raicheva, I.S., *Study of Groundwater Regime at the Sites of the Reference Hydrogeological Network and Representative Basin "Plotnikova-Dalniy",* Long-Term Report on the Study of Groundwater Regime in the Territory of Kamchatka Region for 1986–1990. Report of State Geological Syrvey Kamchatgeologiya, Thermalny, 1993.

Manukhin, Y.F. and Vorozheikina, L.F., Hydrogeology of Paratunsky hydrothermal system and conditions of its formation, in *Hydrothermal Systems and Geothermal Fields of Kamchatka*, DVNC AN USSR, Vladivostok, 1976, pp. 143–178.

Marinkovi´c, G., Case study of mountainous geothermal reservoirs (Kopaonik Mt., southwestern Serbia): Fault-controlled fluid compartmentalization within a late Paleogene-Neogene core-complex, *Geothermics,* 2023, vol. 114, 102 799.
https://doi.org/10.1016/j.geothermics.2023.102799

Masurenkov, Yu.P., *Long-Lived Center of Volcanic Activity in Southern Kamchatka,* Moscow: Nauka, 1980.

Matychenkov, V.E., *Thermomineral Waters of Kyrgyzia, Cand. Sci. (Geol.-Mineral.) Dissertation,* St Petersburg, 1992. 282 p. https://viewer.rsl.ru/ru/rsl01000320578.

Pavlova, L.E., Efremova, L.A., and Novikova, E.V., *Summary Report on the Study of Groundwater Regime in the Kamchatka Region for the Period 1964–1975*, Yelizovo: Kamchatka Territorial Hydrogeological Administration, 1979. 5 vols.

Peiffer, L., Inguaggiato, C., Wurl, J., Fletcher, J., Martínez, M., Martínez, D., Legrand, D., Hernandez-Morales, P., Reinoza, C., Tchamab´e, B., Arana-Salinas, L., and Casarín, R., 2024. Geochemistry of coastal geothermal systems from southern Baja California peninsula (Mexico): Fluid origins, water-rock interaction and tectonics, *Chemical Geology*, 2024, vol. 670, 122 316.
https://doi.org/10.1016/j.chemgeo.2024.122316

Peng, C., Assessment of thermal water and energy recoverable rate based on express method: A case study of Reshuiwei geothermal field, *Geothermics,* 2023, vol. 114, 102 789. 789. https://doi.org/10.1016/j.geothermics.102

PetraSim User Manual, Rockware Inc., 2024, 152 p. rockware.com/downloads/documentation/petrasim/PetraSimManual.pdf.

Pola, M., Fabbri, P., Piccinini, L., and Zampieri, D., Conceptual and numerical models of a tectonically-controlled geothermal system: a case study of the Euganean Geothermal System, Northern Italy, *Central European Geology,* 2015, vol. 58, pp. 129–151. https://doi.org/10.1556/24.58.2015.1-2.9

Polyak, B.G., Lavrushin, V.Yu., Cheshko, A.L., and Kikvadze, O.E. Chesnokov, G.A., Ed. *Termy Chukotki* (Geothermal Occurrences in Chukotka), Moscow: GEOS, 2022.

ISBN 978-5-89118-857-0 *Program Library LIDA-3 for Function Approximation and Digital Filtration of Signals and Images*, Novosibirsk, SO USSR Acad. Sci., 1987.

Pruess, K., Oldenburg, C., and Moridis, G., *TOUGH2 User's Guide, Version 2.0.* Rep. LBNL-43134, Lawrence Berkeley Natl. Lab., Berkeley, California, 1999.

Rajeh, T., Al-Kbodi, B.H., Zayed, M.E., Li, Y., Zhao, J., and Rehman, S., Local entropy generation optimization and thermodynamic irreversibility analysis of oval-shaped coaxial ground heat exchangers: A detailed numerical investigation, *International Journal of Heat and Mass Transfer,* 2024a, vol. 228, 125 650.

Rajeh, T., Al-Kbodi, B.H., Li, Y., Zhao, J., Zayed, M.E., and Rehman, S., Comparative numerical modeling complemented with multi-objective optimization and dynamic life cycle assessment of coaxial ground heat exchangers with oval-shaped and typical circular-shaped configurations, *Applied Thermal Engineering,* 2024b, vol. 244, 122 673.

Schill, E. and Genter, A., 2013. EGS Geothermal challenges within the Upper Rhine Valley based on Soultz experience, in *Proc. Third European Geothermal Review,* Mainz, Germany, June 24–26, 2013, p. 16.

Shvartsev, S.L., Zamana, L.V., Plyusnin, A.M., and Tokarenko, O.G., 2015. Equilibrium of nitrogen-rich spring waters of the Baikal Rift Zone with host rock minerals as a basis for determining mechanisms of their formation, *Geochemistry International,* 2015, vol. 53, no. 8, pp. 713–725. https://doi.org/10.1134/S0016702915060087

Smirnova, N.F., *Report on Final Works on the Upper-Paratunsky Thermal Water Field Carried out in 1980–1981* (Detailed Exploration of the Upper-Paratunsky Thermal Water Field), Paratunsky hydrogeological survey, Thermalny, 1981.

Surmaazhav, D., *Thermal Waters in Hydrogeologic Structures of the Khangai Rise of Central Mongolia, Extended Abstract of Cand. Sci. (Geol.-Mineral.) Dissertation*, Irkutsk, 2021, 164 p. http://www.crust.irk.ru/images/upload/newsfull200/2916.pdf.

Thunderhead Engineering PetraSim User Manual, Rockware, 2023. https://www.rockware.com/downloads/documentation/petrasim/PetraSimManual.pdf.

Tokarev, I., Poturay, V., and Yakovlev, E. Estimation of the thermal water formation at the Kuldur site (Amur region, Russia) according to water isotope composition (2H, 18O), *Environmental Earth Sciences*, 2024, vol. 83:126. https://doi.org/10.1007/s12665-024-11422-7

Torresan, A., Piccinini, L., Pola, M., Zampieri, D., and Fabbri, P., 3D hydrogeological reconstruction of the fault-controlled Euganean Geothermal System (NE Italy), *Engineering Geology*, 2020, vol. 274, 105 740. https://doi.org/10.1016/j.enggeo.2020.105740

Vakin, E.A., The Hydrogeology of Present-Day Volcanic Structures and Hydrothermal Systems in Southeastern Kamchatka, *Extended Abstract of Cand. Sci. (Geol.-Mineral.) Dissertation,* Petropavlovsk-Kamchatskiy, 1968, 250 p.

Yin, H., Zayed, M.E., Li, Y., Yang, L., Fan, Y., Wang, Z., Yin, L., Zhao, J., Hassan Al-Kbodi, B., and Rehman, S., Thermo-economic performance of a leaky downhole coaxial geothermal system for maximizing geothermal energy production: Numerical investigation, *Renewable Energy*, 2024, vol. 232, 121 082.

Zayed, M.E., Shboul, B., Yin, H., Zhao, J., and Zayed, A.A., Recent advances in geothermal energy reservoirs modeling: Challenges and potential of thermo-fluid integrated models for reservoir heat extraction and geothermal energy piles design, *Journal of Energy Storage*, 2023, vol. 62, 106 835.

Zhuravlev, N.B., Conceptual model of thermal supply of low-temperature geothermal field without additional thermal sources, *in Proceedings of the All-Russian Scientific Conference with International Participation "Geothermal Volcanology, Hydrogeology, Geology of Oil and Gas"* (Geothermal Volcanology Workshop 2023), Petropavlovsk-Kamchatsky, IVS FEB RAS, 2023, pp. 37–40.

Zippa, E.V., Geochemistry of Thermal Waters of Jiangxi Province (China), *Extended Abstract of Cand. Sci. (Geol.-Mineral.) Dissertation*, Tomsk, 2020, 126 p. doi earchive.tpu.ru/handle/11683/58046.

Translated by I. Melekestseva